International Journal of Minerals, Metallurgy and Materials
Volume 25, Number 1, January 2018, Page 110
https://doi.org/10.1007/s12613-018-1553-3

Influence of Ag content on the microstructure, mechanical, and tribological properties of TaVN–Ag films

Tong Chen, Li-hua Yu, and Jun-hua Xu

School of Material Science and Engineering, Jiangsu University of Science and Technology, Zhenjiang 212003, China

(Received: 21 April 2017; revised: 3 August 2017; accepted: 9 August 2017)

Abstract: A series of TaVN–Ag nanocomposite films were deposited using a radio-frequency magnetron sputtering system. The microstructure, mechanical properties, and tribological performance of the films were investigated. The results showed that TaVN–Ag films were composed of face-centered cubic (fcc) TaVN and fcc-Ag. With increasing Ag content, the hardness of TaVN–Ag composite films first increased and then decreased rapidly. The maximum hardness value was 31.4 GPa. At room temperature, the coefficient of friction (COF) of TaVN–Ag films decreased from 0.76 to 0.60 with increasing Ag content from 0 to 7.93at%. For the TaVN–Ag films with 7.93at% Ag, COF first increased and then decreased rapidly from 0.60 at 25°C to 0.35 at 600°C, whereas the wear rate of the film increased continuously from 3.91×10^{-7} to 19.1×10^{-7} $mm^3/(N \cdot mm)$. The COF of the TaVN–Ag film with 7.93at% Ag was lower than that of the TaVN film, and their wear rates showed opposite trends with increasing temperature.

Keywords: TaVN–Ag films; RF magnetron sputtering; microstructure; mechanical properties; tribological performances

1. Introduction

TaN-based films have been used as surface-protective materials for cutting tools and wear-resistant parts and in other applications because of their high hardness, good corrosion resistance [1–5], and good chemical stability [6–10]. In recent years, a transition metal or a nonmetallic element has been added to TaN-based films to form multicomponent films with overall enhanced performance. For example, Ju *et al*. [5] added V to NbVSiN films, which improved the films' lubricity at high temperatures by forming V_2O_5.

The testing temperature strongly influences TaVN films. Thus, to expand the applications of TaVN films, their tribological performance at high temperatures should be improved. Ju *et al*. [11] have also reported that Ag added as a soft phase to films can improve their tribological performance at room and intermediate temperatures. Ju and Xu [12] arrived at a similar conclusion in a study of NbN–Ag films.

Mulligan *et al*. [13–15] found that adding Ag to CrN thin films could improve their tribological properties in the temperature range from 25 to 500°C. Aouadi *et al.* [16] prepared VN–Ag films to investigate their lubricious behavior over a wide temperature range. They found that the coefficient of friction (COF) of the films varied from 0.35 at 25°C to 0.15–0.20 at 700–1000°C because of the presence of Ag, V_2O_5, and AgV_xO_y. Shtansky *et al*. [17] studied the tribological performance of MoCN–Ag films and found that they exhibited good lubricious behavior over a wide temperature range because of the presence of Ag, MoO_3, and $AgMo_xO_y$. On the basis of the aforementioned studies, we concluded that the metallic Ag in the films could decrease the COF at low temperatures and that the formation of multiple oxides with Magnéli phase elements could decrease the friction coefficient at high temperatures. We hypothesized that TaVN–Ag films would also show excellent tribological performance; however, no research on the tribological performance of TaVN–Ag films has thus far been reported. In this paper, a series of TaVN–Ag nanocomposite films were deposited using a radio-frequency (RF) magnetron sputtering system. The microstructure, mechanical properties, and tribological performance at different temperatures were investigated.

Corresponding author: Li-hua Yu E-mail: lhyu6@just.edu.cn

2. Experimental

The TaVN–Ag nanofilms were deposited onto AISI 304 stainless steel or Si (100) wafers for different purposes by adjusting the power applied to the Ag target in the magnetron sputtering system. The diameter of the Ta (99.9%), V (99.9%), and Ag (99.9%) targets was 75 mm. RF power sources were used. The polished stainless steel and Si wafers were cleaned sequentially with alcohol, acetone, and again with alcohol. When the vacuum degree reached 6×10^{-4} Pa, nitrogen and argon were introduced into the chamber. The targets were cleaned for 5–10 min. TaVN–Ag films were deposited using a Ta target power of 200 W while varying the Ag target power from 0 to 40 W. The working pressure during the whole process was constant at 0.3 Pa. The nitrogen-to-argon volume ratio of the flow was 10:3. The other experimental parameters are listed in Table 1.

Table 1. Process parameters for TaVN–Ag composite films

Sample No.	Ta target power / W	V target power / W	Ag target power / W	Sputtering pressure / Pa	Ar / (10^{-6} $m^3 \cdot min^{-1}$)	N_2 / (10^{-6} $m^3 \cdot min^{-1}$)
1	200	120	0	0.3	10	3
2	200	120	25	0.3	10	3
3	200	120	30	0.3	10	3
4	200	120	40	0.3	10	3

The phase composition and microstructure of the samples were confirmed by X-ray diffraction (XRD). The samples were scanned on a Shimadzu XRD-600 diffractometer at a scanning rate of 4°/min over the 2θ range from 30° to 80°. To attain the specific elemental contents of different samples, energy-dispersive X-ray spectroscopy (EDS, JSM-6480) analysis was carried out during the process of surface observation by scanning electron microscopy (SEM; JEOL JSM-6480). The grain size was calculated according to the Debye–Scherrer formula.

High-resolution transmission electron microscopy (HRTEM) observations were carried out in a JEOL JEM-2010F microscope operated at an accelerating voltage of 200 kV. The hardness and elastic modulus of the films were obtained using the nanoindenter Nano Hardness Tester-2 (NHT2) + Micro Scratch Tester (MST) supported by CSM Company; the number of testing points was at least eight. Also, we used the samples deposited onto stainless steel to test the tribological properties using a Universal Micro-Tribotester-2 (UMT-2) supported by CETR tribometer. A Bruker 3D profilometer was used to measure the wear tracks to calculate the wear loss (V). The wear rate (W) was calculated according to the following equation [3]:

$$W = \frac{V}{S \times L}$$

where S is the total sliding distance and L is the applied load.

In this work, for structural analyses (XRD and HRTEM) and nanoindentation tests, the samples deposited on Si (100) wafer substrates were used. For tribological tests, the samples deposited on AISI 304 stainless steel substrates were used.

3. Results and discussion

3.1. Structure analysis

Fig. 1 shows the elemental compositions of TaVN–Ag films. As shown in Fig. 1, the Ag content increased from 0 to 7.93at% as the Ag target power was increased from 0 to 40 W.

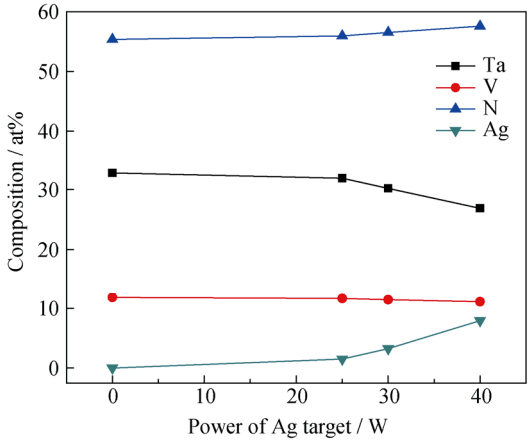

Fig. 1. Compositions of TaVN–Ag films as a function of the Ag target power.

Fig. 2 shows the XRD patterns of the TaVN–Ag films. As shown, the TaVN–Ag films include a face-centered cubic (fcc) TaVN phase with a slight (200) preferential orientation. Similar to other TMN–Ag (TMN: transition-metal nitride) films, no Ag compounds were detected. Laurila *et al.* [18] used a phase diagram to explain that TaN and Ag do not react. Ju *et al.* [12] explained that Ag was dispersed in NbN–Ag thin films in the form of crystals.

Furthermore, Mulligan and Gall [13] investigated the microstructure of CrN–Ag films and found no peaks corresponded to Ag compounds because the Ag content was lower than 12at%.

Fig. 2(b) shows the XRD profile of the TaVN–Ag film in the region from 41.00° to 42.58°, where the data were collected at a low scanning speed. As evident in Fig. 2(b), the diffraction peak shifted to larger angles with increasing Ag content. As evident in Fig. 3, residual compressive stress is present in the TaVN–Ag film. With increasing Ag content, the residual compressive stress of the film gradually increases and the diffraction peak is shifted to larger angles. Kaushal and Kaur have reported similar results [19].

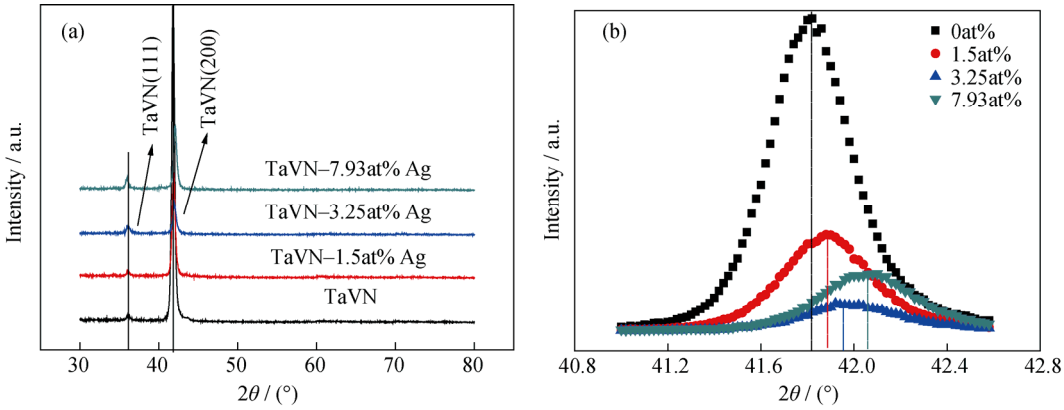

Fig. 2. XRD patterns (a) and a zoomed view of the (200) peaks in the XRD patterns of TaVN–Ag films with different Ag contents (b).

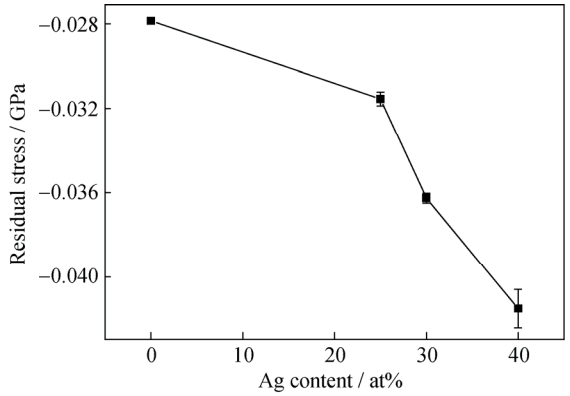

Fig. 3. Residual stress of TaVN–Ag composite films with different Ag contents.

To further study the microstructure of TaVN–Ag films, a TaVN–Ag film with 1.5at% Ag was analyzed by HRTEM; the results are shown in Fig. 4. Three lattice fringes (lattice spacings: ~0.253 nm, ~0.218 nm, ~0.201 nm) are observed. These fringes correspond to fcc-TaVN (111), fcc-TaVN (200), and fcc-Ag (200), respectively. On the basis of the XRD and HRTEM results, the TaVN–Ag film is composed of fcc-TaVN and fcc-Ag phases.

The calculated grain sizes of the TaVN–Ag films are shown in Fig. 5. For the TaVN film, the grain size is ~20.7 nm. For the TaVN–Ag film, the grain size first decreases rapidly and then decreases gradually with increasing Ag content. This behavior is attributed to the added Ag hindering grain growth.

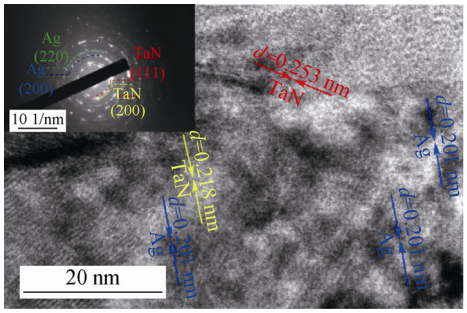

Fig. 4. HRTEM image and selected area electron diffraction (SAED) patterns of TaVN–Ag films with 1.5at% Ag.

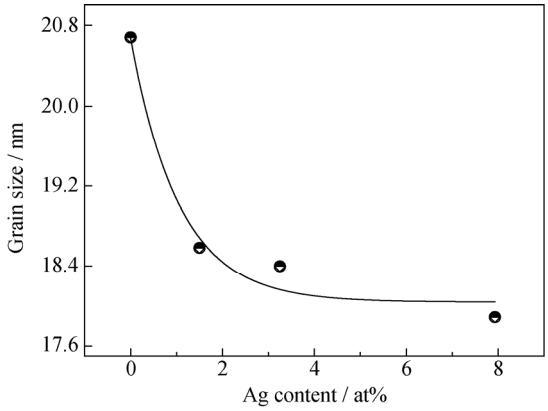

Fig. 5. Grain sizes of TaVN–Ag composite films with different Ag contents.

3.2. Mechanical properties

The nanohardness (H) and elastic modulus (E) of

TaVN–Ag films are presented in Fig. 6. It shows that the H and E of the TaVN film are 30.6 and 378.6 GPa, respectively. With increasing Ag content, the H and E first increase and then decrease rapidly. The maximum values of H and E are 31.4 and 419.4 GPa, respectively, which occur in the case of 1.5at% Ag. In cases where the Ag content is lower than 1.5at%, the hardness enhancement likely resulted from fine grain strengthening [20–21]. In cases where the Ag content exceeds 1.5at%, the softer Ag phase may result in a decrease of H. A decrease in the interface energy will result in the grain boundary sliding easily [22].

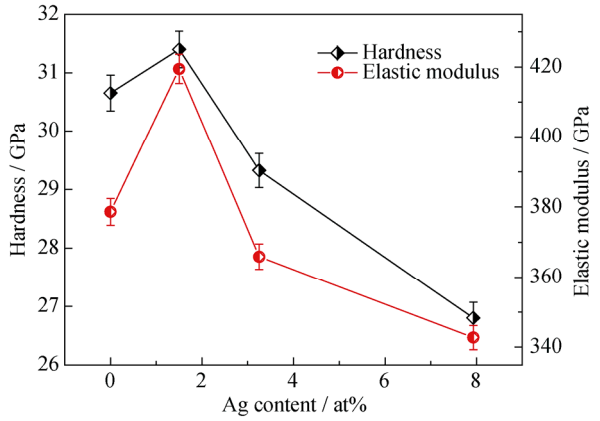

Fig. 6. Hardness and elastic modulus of TaVN–Ag composite films with different Ag contents.

3.3. Tribological performance

Fig. 7 shows the room-temperature COF values of TaVN–Ag films with different Ag contents. The COF of the TaVN film is 0.76. With increasing content of Ag, the COF decreases gradually and reaches a minimum value of 0.60 at an Ag content of 7.93at%. The decrease of the COF is attributed to the presence of soft metal [23]. The soft metal accumulating in the contact area under the heat of friction may also function as a lubricant phase to decrease the friction coefficient [24].

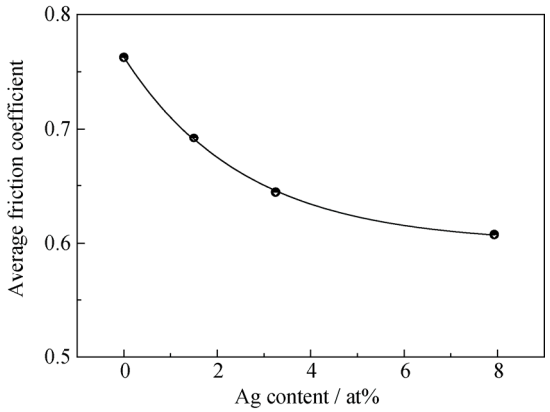

Fig. 7. Room-temperature COF of TaVN–Ag films with different Ag contents.

Fig. 8 shows the average COF and average wear rate of TaVN–Ag with 7.93at% Ag and TaVN films at various temperatures. In Fig. 8(a), with increasing temperature, the COF of TaVN and TaVN–Ag with 7.93at% Ag films first increase and then decrease. The COF of the TaVN–Ag film with 7.93at% Ag is lower than that of the TaVN film under the same conditions. As shown in Fig. 8(b), the wear rates of the TaVN–Ag film with 7.93at% Ag and the TaVN film increase with increasing temperature. The wear rate of the TaVN–Ag film with 7.93at% Ag is higher than that of the TaVN film at the same testing temperature.

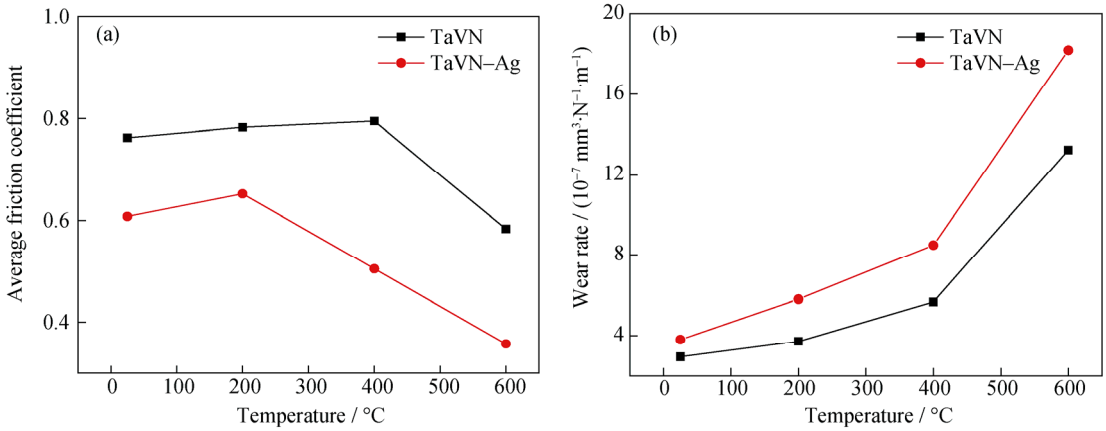

Fig. 8. Average coefficient (a) and wear rate (b) of the TaVN–Ag film with 7.93at% Ag and of TaVN films at different temperatures.

At elevated temperatures, the films might be oxidized, in which case their tribological properties would be influenced by the formed oxides. Thus, to investigate the tribological properties of the films, XRD analyses were conducted. Fig.

9 shows the XRD patterns of the samples of TaVN–Ag films with 7.93at% Ag after sliding tests at different temperatures. As shown, only $AgVO_3$ was detected in the specimen tested at 200°C; Ta_4O was detected in the specimen tested at 400°C. In the specimen tested at 600°C, V_2O_5, $AgTaO_3$, and Ag_3VO_4 were detected.

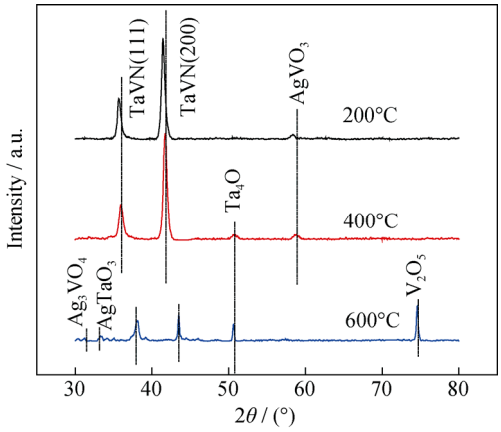

Fig. 9. XRD patterns of TaVN-Ag composite films with 7.93at% Ag after sliding testing with different temperatures.

In cases where the testing temperature is lower than 200°C, the increase in COF of TaVN and TaVN–Ag films is due to the evaporation of water vapor and to damage induced by surface adsorption [11]. At test temperatures from 200 to 400°C, the COF of the TaVN film further increases, whereas that of TaVN–Ag films decreases gradually. In our previous work, the increase in COF of TaVN films was mainly due to the larger size of wear debris compared with the magnitude of contact surface roughness [25–26]. In the case of TaVN–Ag films, the lubricant phase $AgVO_3$ formed in this temperature range, possibly decreasing the COF. The decrease in COF of the TaVN films tested at temperatures from 400 to 600°C is mainly attributed to the formation of the lubricant phase V_2O_5. In the case of TaVN–Ag films, other lubricant phases (e.g., $AgTaO_3$, Ag_3VO_4, and V_2O_5) formed; the COF therefore decreased further. Regardless of the temperature (25–600°C), for TaVN and TaVN–Ag films, the wear rate increase was temperature dependent. Compared with the films, the formed oxides have a larger molar volume, which could lead to the generation of greater internal stress, followed by cracking or peeling. Furthermore, increasing temperature would promote the oxidation of the films. However, the lubrication phases also have a low shear strength, which would lead them to be worn away easily by friction pairs. Compared with TaVN films, more lubrication phases formed on the surface of the TaVN–Ag films at the same testing temperature. In addition, Ag particles could precipitate out and adhere to the friction pairs, which could also increase the wear rate. Thus, the wear rate of the TaVN film is lower than that of the TaVN–Ag films. On the basis of the aforementioned analysis, the Ag dopant improved the lubrication behavior of TaVN films but failed to improve their wear performance.

4. Conclusions

(1) TaVN–Ag films are composed of fcc-TaVN and fcc-Ag.

(2) With the Ag content increasing, the H and E of TaVN–Ag films increased at first and then decreased. The maximum H and E values were 31.4 and 419.4 GPa at 1.5at% Ag, respectively.

(3) At room temperature, the COF of TaVN–Ag films decreased from 0.76 to 0.60 with increasing Ag content.

(4) The COF of TaVN–Ag films decreased from 0.65 at 200°C to 0.35 at 600°C. The COF of TaVN films decreased from 0.79 at 200°C to 0.58 at 600°C. The COF of the TaVN–Ag film was lower than that of the TaVN film at the same temperature. The wear rate of the TaVN–Ag and TaVN films increased with increasing temperature, and the wear rate of the TaVN–Ag film was larger than that of the TaVN films at the same temperature.

Acknowledgements

This work was financially supported by the National Natural Science Foundation of China (Nos. 51374115 and 51574131), Postgraduate Research & Practice Innovation Program of Jiangsu Province (KYCX17-1832), and Research Fund of Jiangsu University of Science and Technology (YCX16S-22).

References

[1] C.C. Liu, M.H. Weng, C.T. Wang, J.H. Chen, Y.C. Chou, and H.W. Yaw, An investigation of structure and wear properties of TiN/NbN films deposited by reactive magnetron sputtering, *Key Eng. Mater.*, 368-372(2008), p. 1310.

[2] M. Akbazadeh, A. Shafyei, and H.R. Salimijazi, Comparison of the CrN, TiN and (Ti, Cr)N PVD coatings deposited by cathodic arc evaporation, *Iran. J. Mater. Sci. Technol.*, 12(2015), No. 1, p. 43.

[3] Z.W. Wu, F. Zhou, Q.W. Wang, Z.F. Zhou, J.W. Yan, and L.K.Y. Li, Influence of trimethylsilane flow on the microstructure, mechanical and tribological properties of CrSiCN coatings in water lubrication, *Appl. Surf. Sci.*, 355(2015), p. 516.

[4] L.H. Yu, Y. Li, H.B. Ju, and J.H. Xu, Microstructure, mechanical and tribological properties of magnetron sputtered

VCN films, *Surf. Eng.*, 33(2017), No. 12, p. 919.

[5] H.B. Ju, L.H. Yu, S. He, I. Asemoah, J.H, Xu, and Y. Hou, The enhancement of fracture toughness and tribological properties of the titanium nitride films by doping yttrium, *Surf. Coat. Technol.*, 321(2017), p. 57.

[6] J.H. Xu, H.B. Ju, and L.H. Yu, Microstructure, oxidation resistance, mechanical and tribological properties of Mo–Al–N films by reactive magnetron sputtering, *Vacuum*, 103(2014), p. 21.

[7] L. Hultman, Thermal stability of nitride thin films, *Vacuum*, 57(2000), No. 1, p. 1.

[8] L.W. Lin, B. Liu, D. Ren, C.Y. Zhan, G.H. Jiao, and K.W. Xu, Effect of sputtering bias voltage on the structure and properties of Zr–Ge–N diffusion barrier films, *Surf. Coat. Technol.*, 228(2013), Suppl. 1, p. S237.

[9] S. Komiyama, Y. Sutou, K. Oikawa, J. Koike, M. Wang, and M. Sakurai, Wear and oxidation behavior of reactive sputtered δ-(Ti,Mo)N films deposited at different nitrogen gas flow rates, *Tribol. Int.*, 87(2015), p. 32.

[10] T.S. Kumar, S.B. Prabu, G. Manivasagam, and K.A. Padmanabhan, Comparison of TiAlN, AlCrN, and AlCrN/TiAlN coatings for cutting-tool applications, *Int. J. Miner. Metall. Mater.*, 21(2014), No. 8, p. 796.

[11] H.B. Ju, L.H. Yu, D. Yu, I. Asempah, and J.H. Xu, Microstructure, mechanical and trobological properties of TiN–Ag films deposited by reactive magnetron sputtering, *Vacuum*, 141(2017), p. 82.

[12] H.B. Ju and J.H. Xu, Microstructure and tribological properties of NbN–Ag composite films by reactive magnetron sputtering, *Appl. Surf. Sci.*, 355(2015), p. 878.

[13] C.P. Mulligan and D. Gall, CrN–Ag self-lubricating hard coatings, *Surf. Coat. Technol.*, 200(2005), No. 5-6, p. 1495.

[14] C.P. Mulligan, T.A. Blanchet, and D. Gall, CrN–Ag nanocomposite coatings: High-temperature tribological response, *Wear*, 269(2010), No. 1-2, p. 125.

[15] C.P. Mulligan, T.A. Blanchet, and D. Gall, CrN–Ag nanocomposite coatings: Tribology at room temperature and during a temperature ramp, *Surf. Coat. Technol.*, 204(2010), No. 9, p. 1388.

[16] S.M. Aouadi, D.P. Singh, D.S. Stone, K. Polychronopoulou, F. Nahif, C. Rebholz, C. Muratore, and A.A. Voevodin, Adaptive VN/Ag nanocomposite coatings with lubricious behavior from 25 to 1000°C, *Acta Mater.*, 58(2010), No. 16, p. 5326.

[17] D.V. Shtansky, A.V. Bondarev, Ph.V. Kiryukhantsev-Korneev, T.C. Rojas, V. Godinho, and A. Fernández, Structure and tribological properties of MoCN–Ag coatings in the temperature range of 25–700°C, *Appl. Surf. Sci.*, 273(2013), p. 408.

[18] T. Laurila, K. Zeng, J.K. Kivilahti, J. Molarius, T. Riekkinen, and I. Suni, Tantalum carbide and nitride diffusion barriers for Cu metallisation, *Microelectron. Eng.*, 60(2002), No. 1-2, p. 71.

[19] A. Kaushal and D. Kaur, Effect of Mg content on structural, electrical and optical properties of $Zn_{1-x}Mg_xO$ nanocomposite thin films, *Sol. Energy Mater. Sol. Cells*, 93(2009), No. 2, p. 193.

[20] H.L. Zhang, J.F. Li, B.P. Zhang, and W. Jiang, Enhanced mechanical properties in Ag-particle-dispersed PZT piezoelectric composites for actuator applications, *Mater. Sci. Eng. A*, 498(2008), No. 1-2, p. 272.

[21] H. Köstenbauer, G.A. Fontalvo, C. Mitterer, and J. Keckes, Tribological properties of TiN/Ag nanocomposite coatings, *Tribol. Lett.*, 30(2008), No. 1, p. 53.

[22] S.Y. Tan, X.H. Zhang, X.J. Wu, F. Fang, and J.Q. Jiang, Effect of copper content and substrate bias on structure and mechanical properties of reactive sputtered CrCuN films, *J. Alloys Compd.*, 509(2011), No. 3, p. 789.

[23] S.M. Aouadi, P. Basnyat, Y. Zhang, Q. Ge, and P. Filip, Grain boundary sliding mechanisms in ZrN–Ag, ZrN–Au, and ZrN–Pd nanocomposite films, *Appl. Phys. Lett.*, 88(2006), No. 2, p. 741.

[24] K.E. Pappacena, D. Singh, O.O. Ajayi, J.L. Routbort, O.L. Erilymaz, N.G. Demas, and G. Chen, Residual stresses, interfacial adhesion and tribological properties of MoN/Cu composite coatings, *Wear*, 278-279(2012), p. 62.

[25] N. Fateh, G.A. Fontalvo, G.A. Gassner, and C. Mitterer, Influence of high-temperature oxide formation on the tribological behaviour of TiN and VN coatings, *Wear*, 262(2007), No. 9-10, p. 1152.

[26] Q. Luo, Temperature dependent friction and wear of magnetron sputtered coating TiAlN/VN, *Wear*, 271(2011), No. 9-10, p. 2058.